Journal of Biomechanics 82 (2019) 397–403

Contents lists available at ScienceDirect

Journal of Biomechanics

journal homepage: www.elsevier.com/locate/jbiomech
www.JBiomech.com

Short communication

# Biomechanics in posture space: Properties and relevance of principal accelerations for characterizing movement control

Alessia Longo [a,b], Thomas Haid [b], Ruud Meulenbroek [a], Peter Federolf [b,*]

[a] Donders Institute for Brain, Cognition and Behaviour P.O. Box 9104, 6500 HE Nijmegen, the Netherlands
[b] Department of Sport Science, University of Innsbruck, 6020 Innsbruck, Fürstenweg 185, Austria

ARTICLE INFO

*Article history:*
Accepted 19 November 2018

*Keywords:*
Principal component analysis PCA
Principal acceleration
Largest Lyapunov exponent LyE
Inertial sensors

ABSTRACT

Human movements, recorded through kinematic data, can be described by means of principal component analysis (PCA) through a small set of variables representing correlated segment movements. The PC-eigenvectors then form a basis in the associated vector space of postural changes. Similar to 3D movements, the kinematics in this posture space can be quantified through '*principal*' positions (PPs), velocities (PVs) and accelerations (PAs). The PAs represent a novel set of variables characterizing neuro-muscular control. The aim of the current technical note was to (i) compare the variance explained by PAs with the variance explained by PPs; (ii) clarify the relationship between PAs and segment accelerations; and (iii) compare variability of the first principal acceleration ($PA_1$) with the local dynamic stability (largest Lyapunov exponent, LyE) of the first principal position ($PP_1$). A PCA was applied on 3D upper-body positions collected by an Xsens inertial sensor system as nineteen volunteers performed a bimanual repetitive tapping task. The main finding revealed that the *PP-explained variance* considerably differed from the *PA-explained* variance, indicating that the latter should be considered when reducing the dimensionality in postural movement analysis through a PCA. Further, the current study formally established that the acceleration curves obtained from differentiating segment positions and from linear combinations of PAs are identical. Finally, a strong correlation, $r(17) = 0.92$, $p < 0.001$, was observed between the cycle-to-cycle variability in $PA_1$ and the LyE calculated for $PP_1$, supporting the notion that PA variability and LyE share some of the information they provide about movement control.



## 1. Introduction

A growing number of biomechanical studies apply principal component analysis (PCA). The main purposes of PCA are (i) to detect patterns of correlated variation in the data and (ii) to reduce the dimensionality in the data, i.e. to describe the system with a small set of orthogonal variables that represent a large fraction of the variance in the data. There are many ways to apply PCA, for example, as a tool for waveform analysis (Deluzio and Astephen, 2007; Robertson et al., 2013), to analyze full movement cycles (Federolf et al., 2013a; Zago et al., 2017c; Eskofier et al., 2013), or to detect synergies in EMG data (Bolger et al., 2016; Ting and Macpherson, 2005).

The current study focuses on the analysis of kinematic data that have been interpreted as a high-dimensional posture vector (Troje, 2002; Daffertshofer et al., 2004; Verrel et al., 2009). Human movement, recorded through kinematic data of body segments, then corresponds to variations in these posture vectors. Expressing 3D postural movements in the PCA-spanned basis of this posture space allows to represent the movement as a linear combination of few, one-dimensional movement patterns sometimes called "principal (postural) movements, PMs" (Federolf et al., 2013b; Federolf et al., 2014). If the data are centered, normalized (e.g. using the mean Euclidean distance (Federolf et al., 2013b), and weighted (Gløersen et al.,2017), then between-subject comparisons of PMs become possible (Haid and Federolf, 2018; Zago et al., 2017a). Furthermore, similar to conventional biomechanics, the kinematics of the postural movements are then defined through "principal positions" $PP_k(t)$ – characterizing the momentary posture, "principal velocities" $PV_k(t)$ – characterizing the change in posture, and "principal accelerations" $PA_k(t)$ – characterizing the accelerations that produce postural changes (Federolf, 2016). The current study is the first to compare explained positional variance with explained acceleration variance.

The PAs are a particularly interesting, novel set of variables that allow to explore kinetic aspects of postural movements, for exam-

* Corresponding author.
*E-mail addresses:* a.longo@donders.ru.nl (A. Longo), Thomas.Haid@uibk.ac.at (T. Haid), r.meulenbroek@donders.ru.nl (R. Meulenbroek), Peter.Federolf@uibk.ac.at (P. Federolf).

https://doi.org/10.1016/j.jbiomech.2018.11.031
0021-9290/

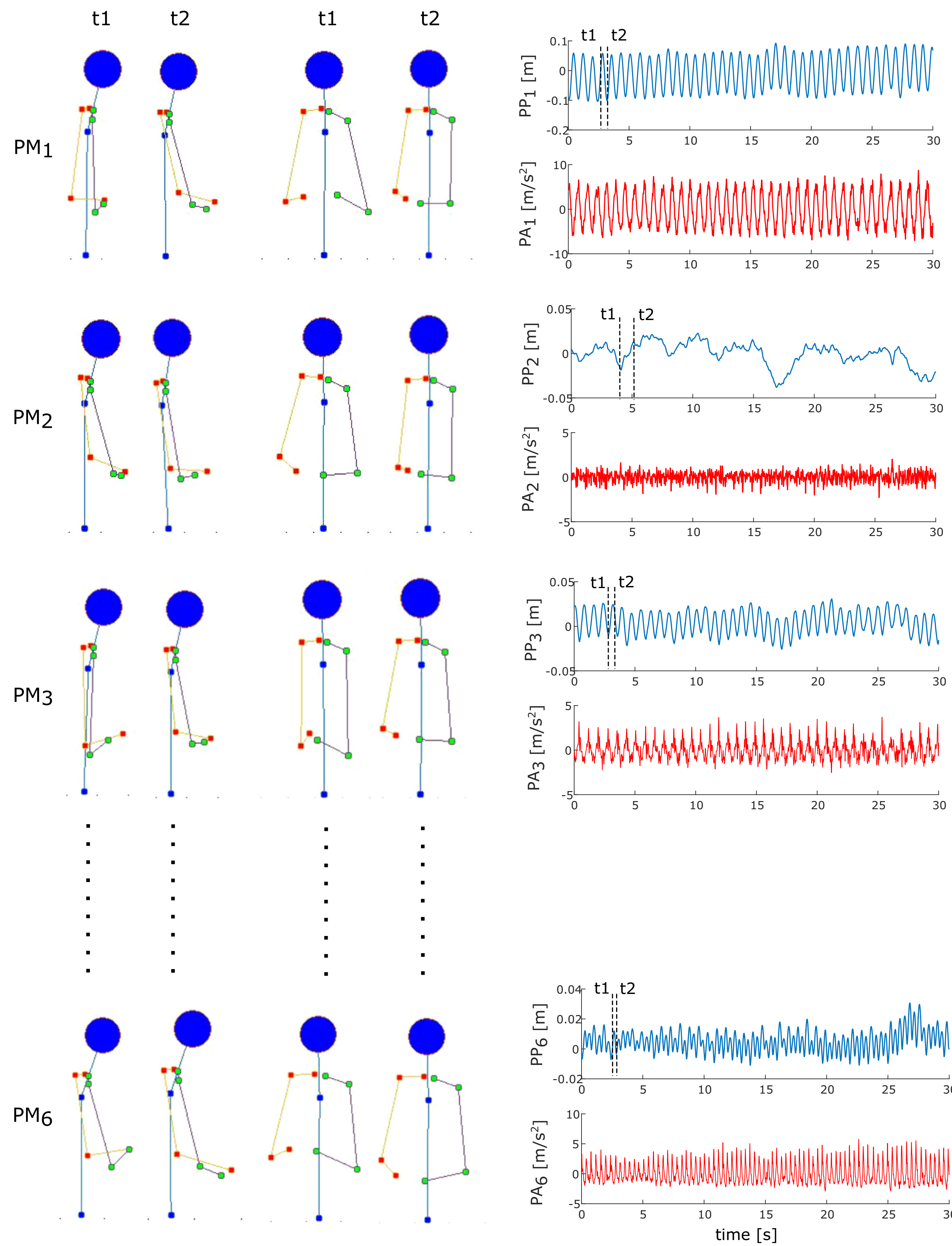


**Fig. 1. Left**: visual representation of the postural changes that $PM_1$, $PM_2$, $PM_3$, and $PM_6$ represent, displayed from 2 perspectives. In each perspective, the left and right images represent the posture at specific time points, t1 and t2, during the movement, corresponding to negative or positive positions on the principal movement. **Right**: Time series for $PM_1$, $PM_2$, $PM_3$, and $PM_6$ displaying the principal position $PP_k(t)$ and principal acceleration $PA_k(t)$. The time points t1 and t2 that were used to create the images on the left are indicated in the $PP_k(t)$ time series. The physical units of the $PP_k(t)$ and $PA_k(t)$ are m and m/s$^2$, respectively; however, please note that these units represent cumulated and normalized segment movements (i.e. distances in posture space). Actual segment movements can be calculated (as done for the graphs on the left side), but cannot be inferred directly from the graphs.

ple, to predict the center of pressure motion from postural movements (Federolf, 2016). Furthermore, since muscles produce (or prevent) posture-changing accelerations, PAs can also be seen as variables reflecting neuro-muscular control (Haid et al., 2018; Promsri et al., 2018). Another point of interest could therefore be to compare the properties of the PAs with other variables used to characterize motor control. For example, the maximum Lyapunov exponent (LyE) is frequently calculated to characterize local dynamic stability of the neuromuscular control system (Dingwell et al., 2001; Stergiou and Decker, 2011). The LyE calculated on the first principal position, $PP_1$ (Federolf et al., 2012; Longo et al., 2018a), should be related to the cycle-to-cycle variability in the first principal acceleration, $PA_1$, since larger LyE, i.e. less predictable movements, imply more variability in the accelerations producing these movements.

The purpose of the current technical note was to (i) compare the acceleration variance explained through the PAs with the variance explained through the PPs; (ii) clarify the relationship between PAs and segment accelerations; and (iii) test the hypothesis that the LyE calculated for $PP_1$ is related to the cycle-to-cycle variability in $PA_1$.

## 2. Method

### 2.1. Participants, procedures and equipment

The data for the current technical note was taken from a previously reported study (Longo et al., 2018b). In brief, nineteen healthy participants [12 females; age 30y (SD: 10.1y)] performed repetitive tapping movements for 15 min between two pairs of targets displayed on a touchscreen (ProLiteIiyama, Iiyama Corporation, Tokyo, Japan). This earlier study proved that PCA is a useful tool in investigating the relationship between postural reconfigurations and pain emerging during the repetitive task (Longo et al., 2018b). All participants provided written informed consent and the study was approved by an institutionalized ethics review board (ECSW2016-2006-405).

An upper-body MVN motion capture system (Xsens technologies BV, Enschede, The Netherlands) consisting of 11 inertial sensors (3D gyroscope, 3D accelerometer and 3D magnetometer) was used to record the kinematics at 60 Hz. Data acquisition was done via the accompanying software (MVN Studio 4.2, Xsens technologies BV, Enschede, Netherlands). The Xsens system was selected for the current study since it provided an output of the full kinematics of each segment: position, velocity, and acceleration. Underlying data processing and filtering are described in (Schepers et al., 2018). The current study used the position and acceleration data of 11 segments: pelvis, T8, head, shoulder (2: left&right), upper arm (2), forearm (2) and hand (2). All further data processing was conducted in Matlab (The MathWorks Inc., Natick, MA, USA).

### 2.2. Data analysis

#### 2.2.1. PCA and kinematics in posture space

A PCA was performed in analogy with previous studies (Troje, 2002; Daffertshofer et al., 2004). The 3D coordinates (x,y,z) of all segments at a given time $t$ were expressed as a posture vector: $\mathbf{p}(t) = [x_1(t), y_1(t), z_1(t), x_2(t), \ldots, y_s(t), z_s(t)]$, where $s$ is the number of segments. The $\mathbf{p}(t)$ were normalized by subtracting the subject-mean $\mathbf{p_n}(t) = \mathbf{p}(t) - {}^{subj}\mathbf{p_{mean}}$. Then the $\mathbf{p_n}(t)$ of all subjects were concatenated into a 342,000 × 33 matrix $\mathbf{P}$ [participants (19) * trial duration (5 min) * measurement frequency (60 Hz) × number of segments (11) * 3D (x,y,z)], whose covariance matrix was decomposed by the PCA algorithm. The PCA provides a set of orthogonal eigenvectors $PC_k$, a set of associated eigenvalues $EV_k$, and a set of scores $PP_k(t)$ [k = order of PM]. The whole set of eigenvectors $PC_k$ form an orthonormal basis in posture space, where each eigenvector $PC_k$ represents a specific pattern of correlated segment movements. The scores $PP_k(t)$ quantify the subject's postural movements (i.e. postural positions as a function of time) with respect to the basis spanned by the associated $PC_k$ (Federolf et al., 2013b). The first and second time derivatives of $PP_k$, $PV_k = \frac{d}{dt}PP_k$ and $PA_k = \frac{d^2}{dt^2}PP_k$, quantify the 'principal velocity' and 'princi-

**Table 1**
Eigenvalues EVk and characterization of the first 6 principal movement components.

| k | Eigenvalue $EV_k$ [%] | Qualitative description of what aspect of the overall movement is predominantly represented in each $PM_k$ |
|---|---|---|
| 1 | 57.77 | Flexion/extension of both shoulders and elbows |
| 2 | 19.33 | Trunk flexion/extension |
| 3 | 7.70 | Shoulders abduction/adduction |
| 4 | 5.37 | Sagittal plane sway of the trunk |
| 5 | 2.48 | Elbows internal/external rotation |
| 6 | 1.91 | Elbows flexion/extension |

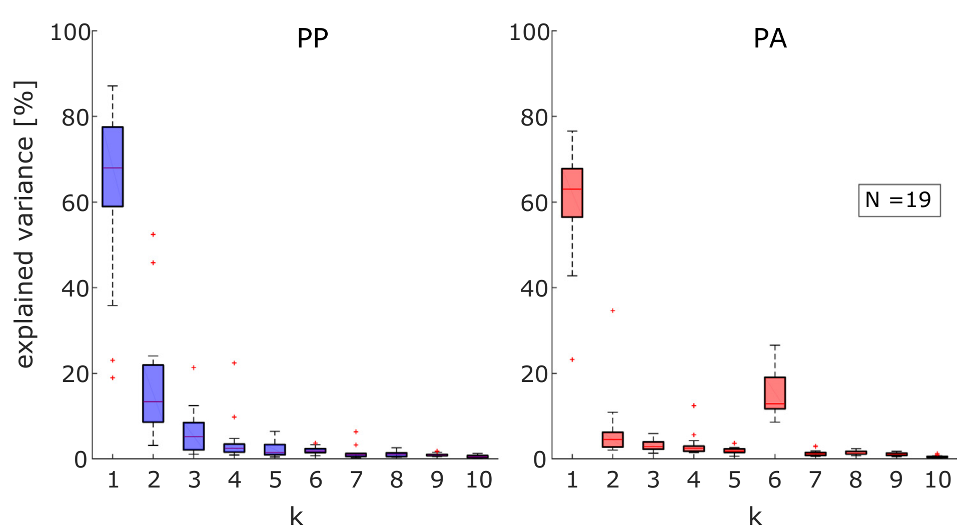


**Fig. 2.** Box plots of the explained relative variance of postural positions, $PP\_rVAR_k$, (left) and explained relative variance of postural accelerations, $PA\_rVAR_k$ (right) observed in the 19 participants. For better clarity, only k = 1 to 10 are displayed (k = order of the principal movement).

pal acceleration' (Fig. 1), respectively. In the current study, the $PP_k$ were not filtered before differentiating, since the Xsens system outputs filtered position data.

*2.2.2. Principal movements and variance explained by $PP_k$ and $PA_k$*

The eigenvalues $EV_k$ calculated through the PCA represent the variance explained by each associated eigenvector. Often the explained variance is considered as a criterion for the decision of how many principal components need to be considered in the analysis (Daffertshofer et al., 2004). In case of concatenated data from several subjects, a subject-specific *explained relative variance*, $PP\_rVAR_k$, can be calculated from the $PP_k$ of each subject (Zago et al., 2017b; Federolf et al., 2013b). In the current study we also calculated the corresponding *explained relative variance for postural*

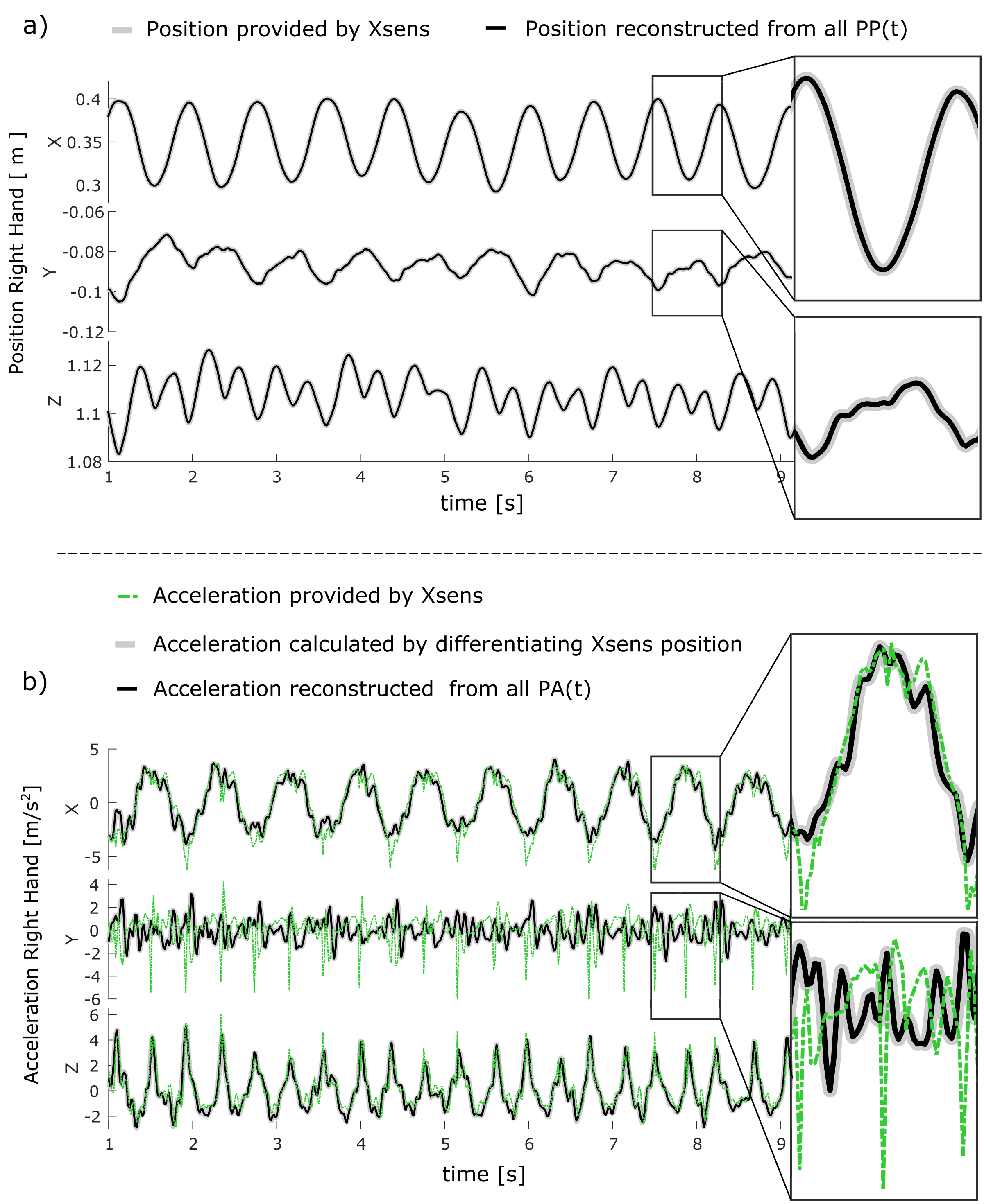


**Fig. 3.** (a) Movement of the right hand segment as described by the original position data provided by Xsens (thick grey line) and reconstructed from the all (k = 1.33) principal positions $PP_k(t)$ (Eq. (1), thin black line) in x,y,z coordinates; (b) acceleration of the right hand segment obtained from differentiating the original Xsens position data (thick grey line); reconstructed from the all principal accelerations $PA_k(t)$ (Eq. (2); thin black line); and, for comparison, the acceleration data provided by the Xsens system (green broken line). (For interpretation of the references to colour in this figure legend, the reader is referred to the web version of this article.)

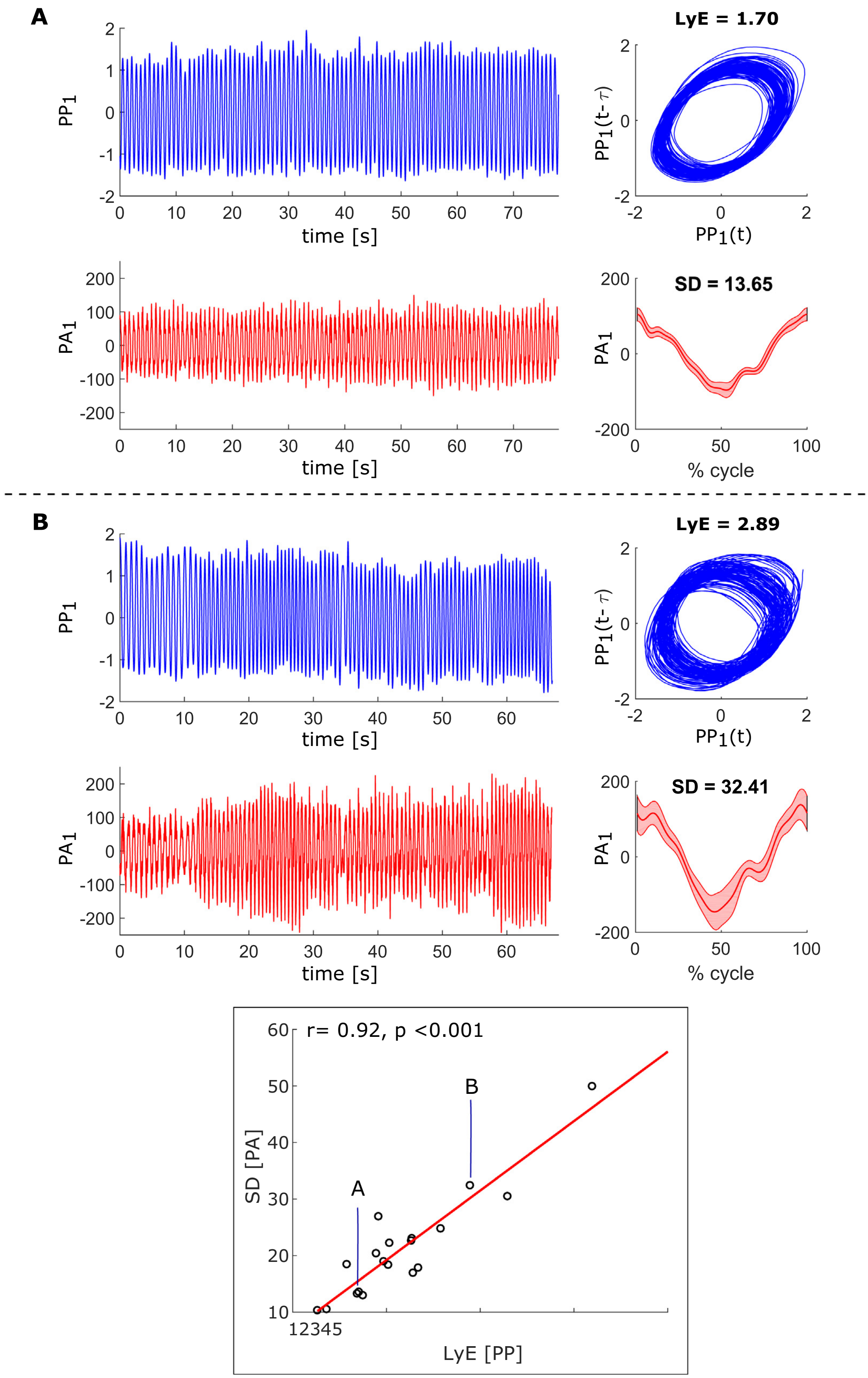


**Fig. 4.** Top two panels: representation of 100-cycles of the first principal position ($PP_1$) over time and its space-time representation for calculation of the Lyapunov exponent (LyE) in blue. Representation of the first principal acceleration ($PA_1$) and the mean ± SD between cycles in red. Two subjects with low (A) and high (B) LyE were selected for this visual comparison. Bottom panel: correlation between mean cycle variability SDc of $PA_1$ and LyE of $PP_1$ using the data from all participants. (For interpretation of the references to colour in this figure legend, the reader is referred to the web version of this article.)

*accelerations*, $PA\_rVAR_k$, i.e. the contribution of each $PA_k$ to the overall acceleration variance of each subject.

*2.2.3. Relationship between segment movements in 3D and PM-movements in postural space.*

Each of the *j* columns in the original posture vector $\mathbf{p}(t)$ represents the position of the specified segment coordinate *j* in 3D space. Hence, at any given time *t* each original segment coordinate can be reconstructed from a linear combination of the scores $PP_k(t)$, the eigenvectors $PC_k$ and the subject-mean ${}^{subj}\mathbf{p}_{\mathbf{mean}}$.

$$p_j(t) = ({}^{subj}\boldsymbol{p}_{mean})_j + \sum_{k=1}^{N} PP_k(t) \cdot PC_{j,k} \tag{1}$$

Similarly, the acceleration of a specific segment coordinate $a_j(t)$ can be expressed as a linear combination of the $PA_k(t)$ and their eigenvectors $PC_{j,k}$

$$a_j(t) = \sum_{k=1}^{N} PA_k(t) \cdot PC_{j,k} \tag{2}$$

A formal derivation of the latter equation is attached in the Supplementary Materials.

*2.2.4. Relationship between PA and LyE*

For each subject, 100 cycles of $PP_1(t)$ were selected. The $PP_1(t)$-amplitude was normalized to unit standard deviation. The amplitude-normalized $PP_1$-time series were also double differentiated to obtain $PA_1$. The Lyapunov exponent (LyE) of $PP_1$ and the between-cycle variability ($SD_C$) of $PA_1$ were calculated for comparisons (Fig. 3). LyE, was calculated by applying Wolf's algorithm (Wolf et al., 1985), which involves a state space representation of the time series (Fig. 3). The time delay ($\tau = 9$) and embedding dimension ($m = 4$) were determined using the average mutual information (AMI; Fraser and Swinney, 1986) and the false nearest neighbor algorithms (Kantz, 1994), respectively. $SD_C$ was determined by first interpolating each cycle (i.e. expressed in percent). Then, for each sample the standard deviation between cycles was determined, and the mean of the standard deviations over the whole cycle was calculated (Fig. 3). Pearson's correlation coefficient r between $SD_C$ of PA1 and LyE of PP1 were evaluated using SPSS Version 22 (IBM, Chicago, IL, USA).

## 3. Results

The first 6 PMs together quantified 94.56% of the overall variance (Table 1) and represented various combinations of arm, shoulder, trunk and head movements (Fig. 1, Table 1). PP_rVAR and PA_rVAR showed substantially different distributions (Fig. 2), specifically, PM6 showed an over-proportional contribution to the participants' postural accelerations.

The mathematical equivalency of segment accelerations $a_j(t)$ with the corresponding vector coefficients *j* in the linear combination of all $PA_k$ (Eq. (2)) was derived in the Supplementary Materials to this paper. As an example, Fig. 3 shows this relationship for the coordinates of the hand sensor: the acceleration curves obtained from the PAs and from a direct differentiation of the position data are identical, however, we observed some deviations from the acceleration raw data exported from Xsens (Fig. 3). Obviously, the Xsens MVN Fusion Engine algorithm applies additional filters in the calculation of the position data (Roetenberg et al., 2013, Schepers et al., 2018).

Finally, we observed a strong correlation $r(17) = 0.92$, $p < 0.001$ between the cycle variability $SD_C$ of $PA_1$ and the LyE of $PP_1$ (Fig. 4), suggesting that the cycle variability in $PA_1$ explained approximately 85% of the variance in the LyEs of $PP_1$.

## 4. Discussion

The most important result of the current study is probably the observation that the *PP-explained variance* and the *PA-explained variance* can exhibit substantially different distributions. This is relevant, because it demonstrates that an additional criterion needs to be considered when reducing the dimensionality in postural movement analysis through PCA: if kinetic aspects of the movement are of interest, then the decision of how many $PM_k$ are considered should be based on both, *PP-* and *PA-explained variance*: there may be movement components that are small in positional amplitude, but are carried out fast enough to considerably influence accelerations and thus forces acting in the system. In the current study, $PM_6$ is an example of such a movement component. Furthermore, this observation also demonstrates that calculating a PCA on position data and then differentiating the PP to obtain PAs (current approach) is not equivalent to first differentiating the positional data to obtain the accelerations of these reference points and then performing a PCA on these accelerations.

In the current study, Xsens data was selected to establish the relationship between PAs and segment accelerations, since the Xsens system directly measures accelerations. When considering data from marker-based motion tracking systems, which determine positional data, noise amplification due to differentiation becomes an additional issue to be considered. In marker-based PA calculations low-pass filters have to be applied (Promsri et al., 2018; Haid et al., 2018). In the current study these filters were implemented in the Xsens motion tracking software (Schepers et al., 2018), but led to differences between differentiated acceleration and the acceleration data provided by Xsens.

Finally, we outlined a possible application of PAs for motor control studies. While the $SD_C$ of the first principal acceleration and the LyE of the first principal position do not quantify exactly the same aspects of the neuromuscular controller, the high correlation suggests that these two variables share a large proportion of the information that they provide. One advantage of assessing movement control with PAs compared to calculating non-linear variables like LyE, entropy, detrended fluctuation analysis, etc. might be that the non-linear calculations require relatively long, stationary time series (Van Emmerik et al., 2016), while PAs can be calculated for every data point. Thus, underlying structures, as visible in the PA time series of Fig. 4B, can be observed. Furthermore, interpreting the structure and properties of the accelerations that produce postural movements might be more intuitive than interpreting results from the aforementioned non-linear methods.

In conclusion, the current technical note highlighted some of the properties of the PAs, which were purported as a new set of variables that could be helpful in investigations into human movement and how it is controlled.

## Conflict of interest statement

The authors have no conflicts of interest

## Acknowledgements

Authors A.L. and R.M. received funding from the European Union FP7 Marie Curie IDP Grant (FP7-PEOPLE-2013-ITN 'Health-PAC', grant 604063-IDP).

## Appendix A. Supplementary material

Supplementary data to this article can be found online at https://doi.org/10.1016/j.jbiomech.2018.11.031.

## References


Bolger, C.M., Sandbakk, Ø., Ettema, G., Federolf, P., 2016. How hinge positioning in cross-country ski bindings affect exercise efficiency, cycle characteristics and muscle coordination during submaximal roller skiing. PLoS One 11, (5). https://doi.org/10.1371/journal.pone.0153078 e0153078.

Daffertshofer, A., Lamoth, C.J.C., Meijer, O.G., Beek, P.J., 2004. PCA in studying coordination and variability: a tutorial. Clin. Biomech. 19 (4), 415–428. https://doi.org/10.1016/j.clinbiomech.2004.01.005.

Deluzio, K.J., Astephen, J.L., 2007. Biomechanical features of gait waveform data associated with knee osteoarthritis: an application of principal component analysis. Gait Posture 25 (1), 86–93. https://doi.org/10.1016/J.GAITPOST.2006.01.007.

Dingwell, J.B., Cusumano, J.P., Cavanagh, P.R., Sternad, D., 2001. Local dynamic stability versus kinematic variability of continuous overground and treadmill walking Retrieved from J. Biomech. Eng. 123 (1), 27–32 http://www.ncbi.nlm.nih.gov/pubmed/11277298.

Eskofier, B.M., Federolf, P., Kugler, P.F., Nigg, B.M., 2013. Marker-based classification of young–elderly gait pattern differences via direct PCA feature extraction and SVMs. Comput. Methods Biomech. Biomed. Eng. 16 (4), 435–442. https://doi.org/10.1080/10255842.2011.624515.

Federolf, P.A., 2016. A novel approach to study human posture control: "Principal movements" obtained from a principal component analysis of kinematic marker data. J. Biomech. 49 (3), 364–370. https://doi.org/10.1016/j.jbiomech.2015.12.030.

Federolf, P.A., Boyer, K.A., Andriacchi, T.P., 2013a. Application of principal component analysis in clinical gait research: identification of systematic differences between healthy and medial knee-osteoarthritic gait. J. Biomech. 46 (13), 2173–2178. https://doi.org/10.1016/J.JBIOMECH.2013.06.032.

Federolf, P., Reid, R., Gilgien, M., Haugen, P., Smith, G., 2014. The application of principal component analysis to quantify technique in sports. Scand. J. Med. Sci. Sports 24 (3), 491–499. https://doi.org/10.1111/j.1600-0838.2012.01455.x.

Federolf, P., Roos, L., Nigg, B.M., 2013b. Analysis of the multi-segmental postural movement strategies utilized in bipedal, tandem and one-leg stance as quantified by a principal component decomposition of marker coordinates. J. Biomech. 46 (15), 2626–2633. https://doi.org/10.1016/J.JBIOMECH.2013.08.008.

Federolf, P., Tecante, K., Nigg, B., 2012. A holistic approach to study the temporal variability in gait. J. Biomech. 45 (7), 1127–1132. https://doi.org/10.1016/j.jbiomech.2012.02.008.

Fraser, A.M., Swinney, H.L., 1986. Independent coordinates for strange attractors from mutual information. Phys. Rev. A 33 (2), 1134–1140. https://doi.org/10.1103/PhysRevA.33.1134.

Gløersen, Ø., Myklebust, H., Hallén, J., Federolf, P., 2017. Technique analysis in elite athletes using principal component analysis. J. Sports Sci. 1–9. https://doi.org/10.1080/02640414.2017.1298826.

Haid, T., Federolf, P., 2018. Human postural control: assessment of two alternative interpretations of center of pressure sample entropy through a principal component factorization of whole-body kinematics. Entropy 20 (1), 30. https://doi.org/10.3390/e20010030.

Haid, T.H., Doix, A.-C.M., Nigg, B.M., Federolf, P.A., 2018. Age effects in postural control analyzed via a principal component analysis of kinematic data and interpreted in relation to predictions of the optimal feedback control theory. Front. Aging Neurosci. 10, 22. https://doi.org/10.3389/fnagi.2018.00022.

Kantz, H., 1994. A robust method to estimate the maximal Lyapunov exponent of a time series. Phys. Lett. A 185 (1), 77–87. https://doi.org/10.1016/0375-9601(94)90991-1.

Longo, A., Federolf, P., Haid, T., Meulenbroek, R., 2018a. Effects of a cognitive dual task on variability and local dynamic stability in sustained repetitive arm movements using principal component analysis: a pilot study. Exp. Brain Res. https://doi.org/10.1007/s00221-018-5241-3.

Longo, A., Meulenbroek, R., Haid, T., Federolf, P., 2018b. Postural reconfiguration and cycle-to-cycle variability in patients with work-related musculoskeletal disorders compared to healthy controls and in relation to pain emerging during a repetitive movement task. Clin. Biomech. 54. https://doi.org/10.1016/j.clinbiomech.2018.03.004.

Promsri, A., Haid, T., Federolf, P., 2018. How does lower limb dominance influence postural control movements during single leg stance? Hum. Mov. Sci. 58, 165–174. https://doi.org/10.1016/j.humov.2018.02.003.

Robertson, G., Caldwell, G., Hamill, J., Kamen, G., Whittlesey, S., 2013. Research methods in biomechanics, 2E. Hum. Kinet., 319–326

Roetenberg, D., Luinge, H., Slycke, P. 2013. Xsens MVN: Full 6DOF Human Motion Tracking Using Miniature Inertial Sensors, 3. Retrieved from https://pdfs.semanticscholar.org/cc2b/a84a4d6e06fd85ad434f5b1a8545c1cc993c.pdf

Schepers, M., Giuberti, M., Bellusci, M. 2018. Xsens MVN Whitepaper: Consistent Tracking of Human Motion Using Inertial Sensing. Document MV0424P.A.

Stergiou, N., Decker, L.M., 2011. Human movement variability, nonlinear dynamics, and pathology: is there a connection? Hum. Mov. Sci. 30 (5), 869–888. https://doi.org/10.1016/j.humov.2011.06.002.

Ting, L.H., Macpherson, J.M., 2005. A limited set of muscle synergies for force control during a postural task. J. Neurophysiol. 93 (1), 609–613. https://doi.org/10.1152/jn.00681.2004.

Troje, N.F., 2002. Decomposing biological motion: a framework for analysis and synthesis of human gait patterns. J. Vis. 2 (5), 2. https://doi.org/10.1167/2.5.2.

Van Emmerik, R.E.A., Ducharme, S.W., Amado, A.C., Hamill, J. 2016. Comparing dynamical systems concepts and techniques for biomechanical analysis. https://doi.org/10.1016/j.jshs.2016.01.013.

Verrel, J., Lövdén, M., Schellenbach, M., Schaefer, S., Lindenberger, U., 2009. Interacting effects of cognitive load and adult age on the regularity of whole-body motion during treadmill walking. Psychol. Aging 24 (1), 75–81. https://doi.org/10.1037/a0014272.

Wolf, A., Swift, J.B., Swinney, H.L., Vastano, J.A., 1985. Determining Lyapunov exponents from a time series. Phys. D: Nonlinear Phenomena 16 (3), 285–317. https://doi.org/10.1016/0167-2789(85)90011-9.

Zago, M., Codari, M., Iaia, F.M., Sforza, C., 2017a. Multi-segmental movements as a function of experience in karate. J. Sports Sci. 35 (15), 1515–1522. https://doi.org/10.1080/02640414.2016.1223332.

Zago, M., Pacifici, I., Lovecchio, N., Galli, M., Federolf, P.A., Sforza, C., 2017b. Multi-segmental movement patterns reflect juggling complexity and skill level. Hum. Mov. Sci. 54, 144–153. https://doi.org/10.1016/J.HUMOV.2017.04.013.

Zago, M., Sforza, C., Bona, A., Cimolin, V., Costici, P.F., Condoluci, C., Galli, M., 2017c. How multi segmental patterns deviate in spastic diplegia from typical developed. Clin. Biomech. 48, 103–109. https://doi.org/10.1016/j.clinbiomech.2017.07.016.